



ELSEVIER

Available online at [www.sciencedirect.com](http://www.sciencedirect.com)

Journal of Magnetism and Magnetic Materials 309 (2007) 171–175

[www.elsevier.com/locate/jmmm](http://www.elsevier.com/locate/jmmm)

# Magnetic semiconducting anatase $\text{TiO}_{2-\delta}$ grown on (1 0 0) $\text{LaAlO}_3$ having magnetic order up to 880 K

Soack Dae Yoon<sup>a,\*</sup>, Yajie Chen<sup>a</sup>, Aria Yang<sup>a</sup>, Trevor L. Goodrich<sup>b</sup>, Xu Zuo<sup>c</sup>,  
Katherine Ziemer<sup>b</sup>, Carmine Vittoria<sup>a</sup>, Vincent G. Harris<sup>a</sup>

<sup>a</sup>Center for Microwave Magnetic Materials and Integrated Circuits, Department of Electrical and Computer Engineering, Northeastern University, Boston, MA 02115, USA

<sup>b</sup>Department of Chemical Engineering, Northeastern University, Boston, MA 02115, USA

<sup>c</sup>College of Information Technical Science, Nankai University, Tianjin 300071, China

Received 12 May 2006

Available online 21 June 2006

## Abstract

We demonstrate a semiconducting material,  $\text{TiO}_{2-\delta}$ , with magnetism up to 880 K, without the introduction of magnetic ions. The magnetism in these films stems from the controlled introduction of anion defects from both the film–substrate interface as well as processing under a deficient oxygen atmosphere. First-principle band structure calculations indicate that the exchange between Ti cations mediated by an oxygen anion is positive, i.e., ferromagnetic, whereas the exchange between cations via a vacancy is negative, i.e., ferrimagnetic. It is likely that both the mechanisms are active in this system. This represents a new and promising approach in the search for room-temperature magnetic semiconductors.

© 2006 Elsevier B.V. All rights reserved.

PACS: 75.50.Dd; 75.50.Pp; 77.55.+f; 85.70.Kh; 61.72.-y; 76.50.+g; 73.50.-h; 73.61.-r; 33.60.Fy

Keywords: Ferromagnetic materials; Semiconductor magnetic; Titanium compounds; Thin films; Defects; Ferromagnetic resonance; Semiconductor transport; X-ray photoelectron spectra

## 1. Introduction

Recent research efforts on the growth of “ferromagnetic” semiconductor materials [1,2] have received great attention because of potential new applications in spintronics devices [3]. The rationale for this optimism is the plausibility of integrating both properties of magnetic and semiconductor materials in new devices [1] (e.g., spin diodes [3–6] and spin-FETs [7]). Recent research has focused on dilute magnetic semiconductors (DMS), which were synthesized by introducing magnetic ions (e.g., Mn, Co, Fe, etc.) into conventional III–V- [1,2] and II–VI-type semiconductors [8,9] or wide bandgap semiconductors including ZnO and  $\text{TiO}_2$  [8–13]. In contrast to previous synthesis approaches, Coey and co-workers [10–12]

reported unexpected magnetism in insulating hafnium dioxide films processed by pulsed laser deposition (PLD) ostensibly by defect doping. This report has created intense debate in the magnetism community as to the origins of magnetism in the Hf-dioxide film system [14–16].

We chose a starting material of anatase  $\text{TiO}_{2-\delta}$  and systematically introduced oxygen defects during the growth process. The  $\text{TiO}_2$  material is known to be a wide bandgap semiconductor. Although stoichiometric  $\text{TiO}_2$  contains only  $\text{Ti}^{4+}$  ions and is non-magnetic,  $\text{Ti}^{3+}$  and  $\text{Ti}^{2+}$  ions can potentially cause magnetism. This requires the Ti ions to be stripped of electrons from s band rather than the 3d band. This, for example, results in  $\text{Ti}^{3+}$  having a  $3d^1$  electronic configuration and  $\text{Ti}^{2+}$  having a  $3d^2$  configuration. As is well known, oxygen vacancies create a charge imbalance and, therefore, a deviation from stoichiometric  $\text{TiO}_2$  with the potential to generate  $\text{Ti}^{3+}$  and  $\text{Ti}^{2+}$  ions. The basic undertaking in this paper is to demonstrate the

\*Corresponding author. Tel./fax: +1 617 373 4853.

E-mail address: [syoon@ece.neu.edu](mailto:syoon@ece.neu.edu) (S.D. Yoon).

ability to control the concentration of oxygen defects and to explore their relationship to magnetism and transport in this oxide semiconductor. The anatase  $\text{TiO}_2$  provides an interesting test bed for these studies because in this structure the Ti cations form a  $156^\circ$  bond angle through the oxygen anion which favours a superexchange interaction with high transition temperatures [17].

Oxygen defects may originate at the interface between the anatase  $\text{TiO}_2$  film and the rhombohedral structure of the (100)-oriented lanthanum aluminate ( $\text{LaAlO}_3$ ) [18] or by the processing of  $\text{TiO}_{2-\delta}$  films in an oxygen-deficient atmosphere. We have explored both the approaches.

Here we report a saturation magnetization,  $4\pi M_S$ , equal to 400 G was measured at room temperature for films grown at an oxygen pressure of 0.3 mTorr. The saturation magnetization versus temperature for this film revealed a transition temperature near 880 K. The magnetization was also found to vary near-linearly with the inverse of film thickness, with the largest values corresponding to thinner films. It is illuminating that the film conductivity scaled with the magnetization suggests that both the spin concentration and charge carrier density are proportional to the electrons generated by the change in Ti valence. This is strong evidence that magnetism arises from a double exchange mechanism.

## 2. Experimental

PLD was employed to deposit 400 nm  $\text{TiO}_{2-\delta}$  films on (100)  $\text{LaAlO}_3$  substrates from rutile  $\text{TiO}_2$  targets under oxygen ambient pressures varied from 0.3 to 400 mTorr. A second series of films having thicknesses of 200–2000 nm were deposited under a fixed oxygen pressure of 0.3 mTorr. Room-temperature stable rutile  $\text{TiO}_2$  targets were prepared by conventional ceramic processing and used as ablation targets for PLD processing of anatase  $\text{TiO}_{2-\delta}$  films. The  $\text{LaAlO}_3$  substrates were measured to be diamagnetic at 300 K. The target of  $\text{TiO}_2$  was 99.8% pure with no magnetic impurities detected by energy-dispersive X-ray spectroscopy (EDXS). The rutile target was measured to be paramagnetic at 300 K. The target was ablated using an KrF excimer laser ( $\lambda = 248$  nm) with the substrate temperature fixed at  $700^\circ\text{C}$ . The laser output energy density was  $200\text{ mJ/cm}^2$ . All samples were handled with tungsten tweezers to eliminate this as a source of magnetic contamination.

Samples were characterized for their structural, magnetic, chemical, and transport properties. The room-temperature DC magnetic properties were measured by vibrating sample magnetometry for all samples up to fields of 12.5 kOe. Select samples were measured over a temperature range of 77–750 K. Ferromagnetic resonance (FMR) was measured on the  $\text{TiO}_{2-\delta}$  films using a  $\text{TE}_{102}$  mode cavity at X-band frequency (9.61 GHz). Structural properties, i.e., lattice parameters and phase identification, were determined by  $\theta$ – $2\theta$  X-ray diffraction (XRD) measurements while chemical analysis was performed using

EDXS, Auger electron spectroscopy (AES), and X-ray photoelectron spectroscopy (XPS). XPS was performed using a PHI 04-173-0-077 Mg/Al dual anode X-ray source with a PHI 10-360-4-015 hemispherical analyser. All data were collected using the Mg anode (1253.6 eV), although an Al anode (1486.6 eV) scan was used to identify Auger peaks from elemental peaks. The integrated Shirley method was used for background subtraction, and curve fitting was performed using RBD Analysis Suite. Depth profile on a  $4\text{ mm} \times 4\text{ mm}$  area was performed using an Ar ion gun at 1–3 keV source voltages and 25 mA with a gun pressure 10 mPa.

Thin films' conductivities were measured at room temperature using the four-points probe technique. DC Hall effect measurements of select samples from 4 to 300 K allowed the determination of carrier type and density.

## 3. Results

$\text{TiO}_{2-\delta}$  films on the (100)  $\text{LaAlO}_3$  substrates were measured by  $\theta$ – $2\theta$  XRD (Cu  $K_\alpha$  radiation). These data, shown in Fig. 1, reveal only the (004) and (008) peaks consistent with the  $c$ -axis orientation of anatase crystals. The lattice mismatch between the anatase  $\text{TiO}_{2-\delta}$  and the  $\text{LaAlO}_3$  substrate is  $-0.26\%$ . The  $c$ -axis lattice parameter, determined by peak profile fitting of  $(00l)$  peaks, was  $0.950 \pm 0.0017$  nm, which compares favourably with  $0.952 \text{ \AA}$  for the bulk anatase structure of  $\text{TiO}_2$  [19]. As seen there are clear distinctions between the position and amplitude of the anatase peaks and those of the rutile and substrate diffraction spectra.

Room-temperature conductivity of  $\text{TiO}_{2-\delta}$  films were measured to range from  $\sim 18$  to  $\sim 0.03 \Omega^{-1}\text{ cm}^{-1}$  for films deposited at 0.3 and 10 mTorr oxygen pressure ( $P_{\text{ox}}$ ),

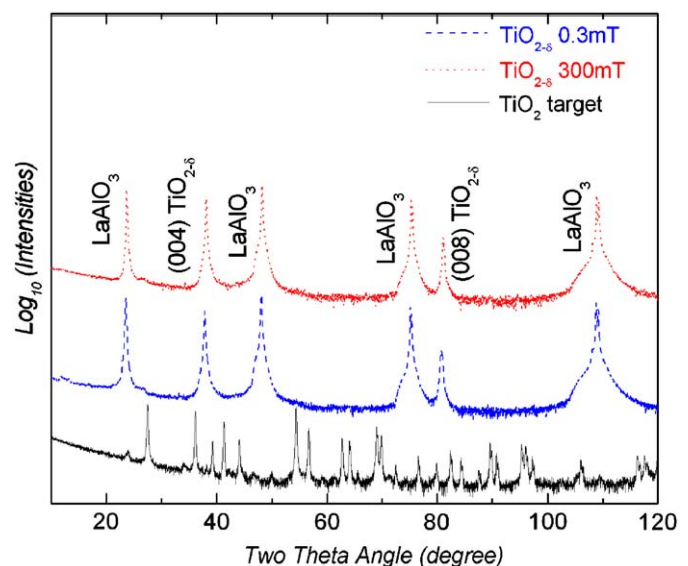


Fig. 1. X-ray diffraction spectra of  $\text{TiO}_{2-\delta}$  films and target material. Blue and red lines correspond to data from films deposited at 0.3 and 400 mTorr, respectively. Similar data are provided for the rutile  $\text{TiO}_2$  target material (black).

respectively. The  $\text{TiO}_{2-\delta}$  films deposited at higher than 10 mTorr of  $P_{\text{ox}}$  showed near-insulating behaviour at room temperature.

The static magnetic properties of the  $\text{TiO}_{2-\delta}$  films at room temperature were measured with the magnetic field applied parallel to the film plane. The saturation magnetization was measured to be  $410 \pm 30$  G, the coercive field was 100 Oe, and remanent magnetization was equal to  $67 \pm 7$  G (see Fig. 2). Several samples showing magnetization were reproduced. In one instance ( $P_{\text{ox}} = 0.3$  mTorr), a total of five samples were deposited with an average  $4\pi M_s$  of 410 G. Magnetic moment as a function of temperature was measured from 77 to 750 K on a film deposited under an oxygen pressure of 0.3 mTorr. The film was magnetically saturated with an applied field of 2 kOe (in plane). From the plot of moment versus temperature (see Fig. 3), the magnetic transition temperature was estimated to be  $\sim 880$  K and the fitted saturation magnetization,  $4\pi M_s$ , at 0 K was 540 G. We have used mean field [19,20] approximation,  $4\pi M_s \sim A 4\pi N \mu (1 - T/T_c)^\beta$ , where  $N$  is electron spin density,  $\mu$  is the Bohr magneton, and  $A$  is an arbitrary constant, to fit the temperature-dependent saturation magnetization (Fig. 3). Fig. 3 shows an unexpected second transition at lower temperatures as is evidenced by the kink appearing around 450 K. Because of this, the data were fit to two functions, one above and one below 450 K. The critical exponent ( $\beta$ ), predicted by mean field theory to be  $\sim 0.5$  [20]. In this manner, we determined a magnetic ordering temperature of 880 K (and a second transition temperature of  $\sim 600$  K). Ferromagnetic resonance (FMR) was measured on the  $\text{TiO}_{2-\delta}$  films using a TE<sub>102</sub> mode cavity at X-band frequency (9.61 GHz). The FMR power derivative linewidth,  $\Delta H$ , at 9.61 GHz was measured to be on the order of  $\sim 2$  to 3 kOe consistent with a defected  $\text{TiO}_{2-\delta}$  structure.

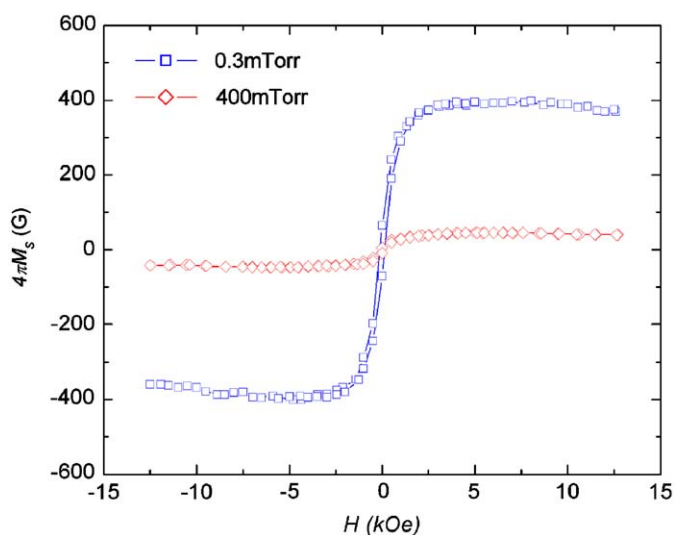


Fig. 2. Magnetic hysteresis loops for  $\text{TiO}_{2-\delta}$  films deposited by PLD at the denoted oxygen pressures. Applied field was aligned parallel to the film plane.

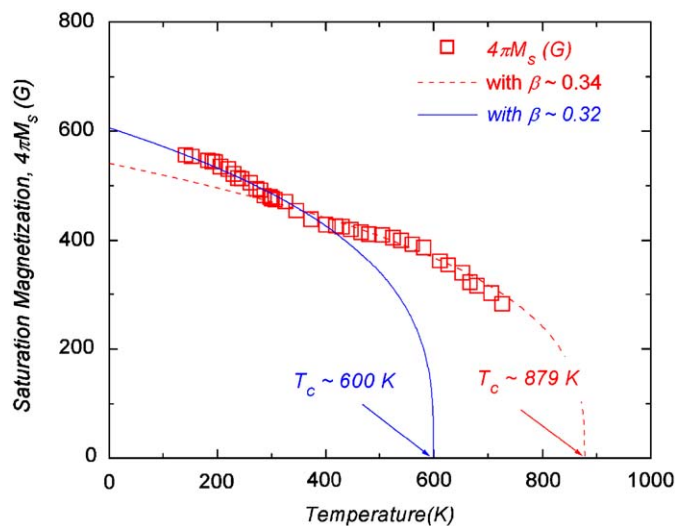


Fig. 3. The temperature dependence of the magnetization for the  $\text{TiO}_{2-\delta}$  film deposited at 0.3 mTorr of oxygen pressure.

If one were to assume that each oxygen defect results in a vacancy, in order to balance the charge around the defect, either one Ti ion must change its valence state from  $4+$  to  $2+$  or two Ti ions must change to  $3+$ . Clearly, the  $\text{Ti}^{3+}$  or  $\text{Ti}^{2+}$  potentially can give rise to magnetism, since they represent  $3d^1$  and  $3d^2$  electronic configurations, respectively. In an early paper, Senftle, Pankey, and Grant [21] attributed an enhanced magnetic susceptibility in bulk anatase  $\text{TiO}_2$  to the presence of trivalent Ti cations. If the density of these defects is low, such that each  $\text{Ti}^{2+}$  or  $\text{Ti}^{3+}$  site is isolated, then one would expect paramagnetism to result. In fact, targets of  $\text{TiO}_2$ , likely to include significant defect concentrations, exhibit paramagnetism. However, if the density of divalent and trivalent Ti cations is increased such that they interact via the super-exchange mechanism, one would then expect ferri- or ferromagnetism to result.

The number of net spins which give rise to the measured magnetization (at 0 K) can be approximated from:  $M(0) \approx Ng\mu_\beta S$ , where  $N$  is the number of net spins between the super-exchange sites. This is also an approximate measure of the number of defects or the number of super-exchange interactions occurring in the film. ( $S$  is the spin at  $T = 0$  K assuming the orbital contribution is negligible). The value of  $S$  can be either  $1/2$  or  $1$  which can result in an error of 2 in our estimate;  $g$  is the splitting  $g$ -factor and  $\mu_\beta = 9.27 \times 10^{-21}$  erg/Oe. We estimate  $N$  to be  $\sim 4 \times 10^{21}$  spins/cm<sup>3</sup>.

To further illuminate the origins of magnetism in this system, we have carried out first-principle band structure calculations. In the computation, the density functional method is Hartree–Fock plus correlation with PWGGA correction [22] and the basis sets are Gaussian-type functions. As the carrier density ( $n$ ) is much lower than the spin density ( $N$ ), most spins should be localized. As a result, the  $\text{Ti}^{3+}$  ions are in close proximity to oxygen vacancies, and the magnetic interactions between these Ti cations ions are short-range super-exchange interactions.

This enables us to compute the exchange interactions using the non-periodic cluster. For the case of  $\text{Ti}^{3+}$  cations that form bond angles through oxygen anions of  $\sim 180^\circ$ , a ferromagnetic exchange results with a Curie temperature near room temperature ( $\sim 360$  K). Alternatively, for Ti cations that interact through a vacancy the exchange is negative, i.e. antiferro- or ferrimagnetic, with a Neél temperature of several 1000 K.

The measured magnetization versus temperature curve of Fig. 3 reveals two magnetic transitions, one near 600 K, and the other at  $\sim 880$  K. We postulate that the lower temperature transition corresponds with the  $T_c$  of the ferromagnetic exchange (Ti cations exchanged coupled through oxygen), while the higher temperature transition is the Neél transition of those sites ferrimagnetically coupled. This is in accordance with the results of the band structure calculations although further studies are required to clarify this assertion.

DC Hall effect measurements performed at temperatures from 4 to 300 K showed the films to be *n*-type semiconductors with a carrier density of  $\sim 3 \times 10^{17}/\text{cm}^3$  at room temperature. The d-band is near the bottom of the conduction band, thus, if the vacancy level is close to the bottom of the conduction band, the system is *n*-type semiconductor where the carriers are d electrons.

Fig. 4 depicts the room-temperature magnetization of the anatase films as a function of the oxygen processing pressure from 0.3 to 400 mTorr. It is clear from these data that a strong relationship exists between magnetization and oxygen pressure, i.e., the magnetization increases rapidly for low oxygen pressures. This suggests that the number of anion defects, or conversely, the density of  $\text{Ti}^{3+}$  and  $\text{Ti}^{2+}$  cations, increases with a reduced oxygen processing pressure. In addition, if anion defects are generating *n*-type carriers one would expect the conductivity to increase. Such is the case, as we measure a logarithmic increase in the conductivity of films deposited at low pressures (see Fig. 4).

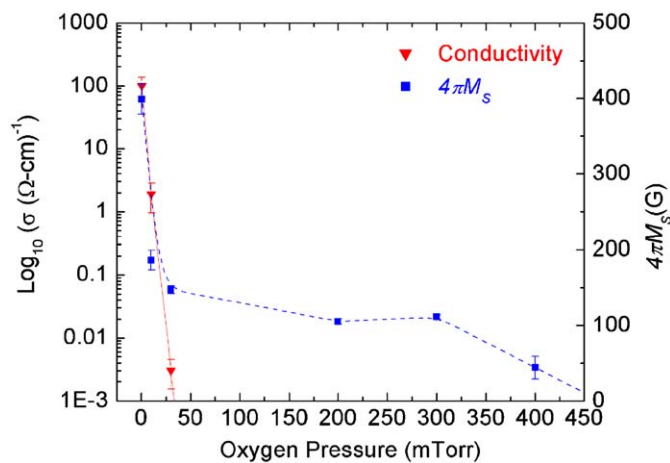


Fig. 4. Room-temperature saturation magnetization (as  $4\pi M_s$ ) and conductivity as a function of oxygen processing pressure.

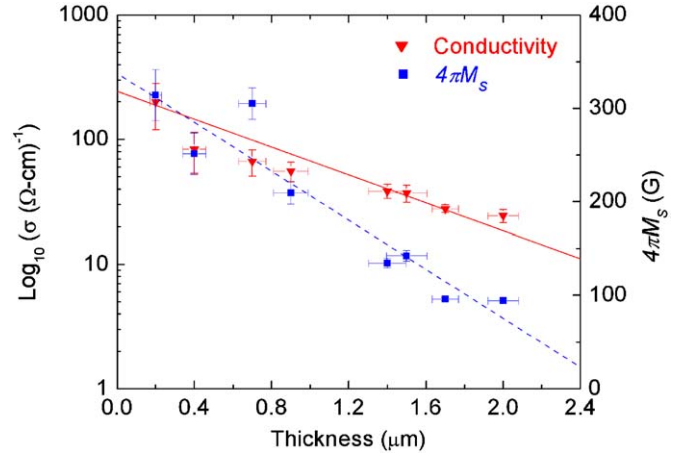


Fig. 5. Room-temperature conductivity as a function of  $\text{TiO}_{2-\delta}$  film thickness grown at 0.3 mTorr of oxygen pressure.

In the report by Venkatesan et al., the magnetism measured in insulating  $\text{HfO}_{2-\delta}$  films was attributed to a polarizing of the impurity band by the 5d band brought about by interfacial defects originating from the lattice mismatch between film and substrate. To explore if this mechanism is active in this system, a second series of films were deposited at a fixed oxygen pressure but at varying thicknesses. If indeed interfacial defects contribute to the magnetism in the  $\text{TiO}_{2-\delta}$  films, then one would expect that the effect would increase for thin samples and reduce for thicker films as the film relaxes to an unstrained state. Recently, the interfacial properties of anatase  $\text{TiO}_{2-\delta}$  grown on the rhombohedral (100)  $\text{LaAlO}_3$  were reported<sup>17</sup>. In that report, it was found that the atomic mismatch at the  $\text{TiO}_{2-\delta}$  film interface generated oxygen vacancies. In this mechanism, the defects provide a means to mediate the strain arising from the lattice mismatch at the interface. Due to these defects, the valence of the Ti ions change to maintain local charge balance. In fact, the semiconductor properties of anatase  $\text{TiO}_2$  stems from just this sort of mechanism. Hence, the transport properties of our defected films should reflect changes in defect concentration as well as potentially the magnetization. In fact, Fig. 5 reveals a systematic trend of increasing magnetization with increasing conductivity for decreasing  $\text{TiO}_{2-\delta}$  film thickness. This is strong evidence that there indeed exists interfacial oxygen defects in the  $\text{TiO}_{2-\delta}$  films on (100)  $\text{LaAlO}_3$  substrates that contribute to both transport and magnetism.

#### 4. Impurities and contaminations

EDXS, AES, and XPS measurements were performed to determine the level of magnetic impurities, namely Ni, Co, and Fe ions, present in these films. Measurements of our most magnetic films found impurity levels were below 0.1%, which was the threshold of resolution for the EDXS and AES measurements. We considered two possible impurity conditions: the impurities may not have oxidized

during deposition and exist as metallic clusters, or the impurities have oxidized where they may exist as substitutional, interstitial or cluster defects. As a metallic impurity, only pure iron has sufficient magnetic moment to account for the measured magnetization. Since the saturation magnetization of metallic iron is about 20 kG at room temperature, a 0.1% Fe impurity level would provide a magnetization of 200 G at room temperature. However, FMR measurements revealed no traces of metallic Fe, although as many as  $\sim 10^{17}$  Fe spins would be present at that level of impurity. Secondly Auger and XPS measurements revealed no traces of Fe in the films. Finally, the films were deposited at above 700 °C in our oxygen atmosphere, and it would be expected that metallic Fe would have oxidized.

Isolated impurities of oxides of FeO, Fe<sub>2</sub>O<sub>3</sub>, NiO, and CoO would not contribute significantly to the measured moment, since their moments is much smaller than pure metallic Fe. However, one can imagine a situation where these ions occupy Ti sites with localized anatase coordination. These types of oxide clusters could contribute to the measured magnetization of the films. Again XPS and AES revealed no measurable presence of these oxide impurities.

Finally, the source for these impurities may be presented in the target material or mechanical handling of the films, such as the use of magnetic tweezers, and/or substrate material. Our films were handled with non-magnetic tungsten tweezers. EDXS and AES measurements revealed no presence of impurities of Ni, Co, and Fe above the 0.1% threshold in the target materials as well as in the substrates. Electron paramagnetic resonance (EPR) measurements on substrates revealed no features attributable to paramagnetic excitations of these oxides. We conclude that the levels of impurities are too low to account for the measured magnetic properties in these films.

## 5. Conclusions

We have demonstrated a systematic technique whereby, for example the semiconductor anatase TiO<sub>2</sub>, when processed with anion defects exhibits both magnetic and semiconducting properties at temperatures near 880 K.

The room-temperature carriers are *n*-type with  $n \sim 3 \times 10^{17} \text{ cm}^{-3}$ . The density of spins is  $\sim 10^{21} / \text{cm}^{-3}$ . The defects were introduced via the substrate lattice mismatch and by processing in an oxygen-deficient atmosphere. First-principle band structure calculations indicate that both ferro- and ferrimagnetism may be present with magnetic ordering temperatures well above room temperature. This represents a new approach in the design and refinement of magnetic semiconductor materials for spintronics device applications.

## Acknowledgements

This research was supported, in part, from the US Office of Naval Research and the US National Science Foundation.

## References

- [1] H. Ohno, *Science* 281 (1998) 951.
- [2] A.H. Macdonald, P. Schiffer, N. Samarth, *Nat. Mater.* 4 (2005) 195.
- [3] G. Prinz, *Science* 282 (1998) 1660.
- [4] R. Fiederling, et al., *Nature* 402 (1999) 787.
- [5] Y. Ohno, et al., *Nature* 402 (1999) 790.
- [6] B.T. Jonker, et al., *Phys. Rev. B* 62 (2000) 8180.
- [7] Supriyo Datta, Biswajit Daset, *Appl. Phys. Lett.* 56 (1990) 665.
- [8] Yuji Matsumoto, et al., *Science* 291 (2001) 854.
- [9] T. Fukumura, et al., *Appl. Phys. Lett.* 78 (2001) 958.
- [10] M. Venkatesan, C.B. Fitzgerald, J.M.D. Coey, *Nature* 430 (2004) 630.
- [11] J.M.D. Coey, et al., *Phys. Rev. B* 72 (2005) 024450.
- [12] J.M.D. Coey, *J. Appl. Phys.* 97 (2005) 10D313.
- [13] S.D. Yoon, et al., *J. Appl. Phys.* 99 (2006) 08M109.
- [14] D.W. Abraham, M.M. Frank, Supratik Guha, *Appl. Phys. Lett.* 87 (2005) 252502.
- [15] Wendong Wang, et al., *J. Appl. Phys.* 99 (2006) 08M117.
- [16] M. Ramachandra Rao, et al., *Appl. Phys. Lett.* 88 (2006) 142505.
- [17] P.W. Anderson, *Phys. Rev.* 102 (1956) 1008.
- [18] A. Sasahara, et al., *Nanotechnology* 16 (2005) S18.
- [19] C.J. Howard, T.M. Sabine, F. Dickson, *Acta Crystallogr. Sect. B: Struct. Sci.* B 47 (4) (1991) 462.
- [20] L.P. Kadanoff, et al., *Rev. Mod. Phys.* 39 (1967) 395.
- [21] F.E. Senftle, T. Pankey, F.A. Grant, *Phys. Rev.* 120 (1960) 820.
- [22] J.P. Perdew, Kieron Burke, Matthias Ernzerhof, *Phys. Rev. Lett.* 77 (1996) 3865.